http://dx.doi.org/10.5935/0103-5053.20150180

J. Braz. Chem. Soc., Vol. 26, No. 10, 2003-2013, 2015.
Printed in Brazil - ©2015 Sociedade Brasileira de Química
0103 - 5053 $6.00+0.00

Article

Preparation of a Nitrite Electrochemical Sensor Based on Polyaniline/ Graphene-Ferrocenecarboxylic Acid Composite Film Modified Glass Carbon Electrode and its Analytical Application

Yuli Wei,[a,b] Fang Fang,[a] Wu Yang,[a] Hao Guo,[a] Xiuli Niu[a] and Lijun Sun[c]*

[a]*Key Lab of Bioelectrochemistry and Environmental Analysis of Gansu Province, College of Chemistry and Chemical Engineering, Northwest Normal University, 730070 Lanzhou, P. R. China*

[b]*Petrochemical Research Institute, Lanzhou Petrochemical Research Center, PetroChina, 730060 Lanzhou, P. R. China*

[c]*Petrochemical Reseach Institute, PetroChina, 100195 Beijing, P. R. China*

A sensitive and stable electrochemical sensor based on polyaniline/graphene-ferrocenecarboxylic acid (PANI/GR-FCA) composite film modified glass carbon electrode for determination of nitrite was presented and its morphology and structure were characterized by scanning electron microscope (SEM), transmission electron microscope (TEM), Fourier transform infrared spectroscopy (FTIR) and X-ray powder diffraction (XRD). Cyclic voltammetry (CV) and differential pulse voltammetry (DPV) techniques were used to investigate the electrochemical behavior of the nitrite oxidation, which exhibited an enhanced voltammetric response at the modified electrode. In the optimal condition, the oxidation of nitrite in Britton-Robinson buffer solution (BR) of pH 4.0 had the higher peak current than the bare electrode. A linear calibration curve over the concentration range 0.4-300 μmol L^{-1} of nitrite were obtained with a linear regression equation I (μA) = 0.1589 + 0.0020C (μmol L^{-1}) (R = 0.9991, n = 13) and the detection limit was down to 0.02 μmol L^{-1} (S/N = 3). The recoveries of all determinations ranged between 96-102%. At the same time, the modified electrode showed a good long-term stability and reproducibility for determination of nitrite, as well as high selectivity.

Keywords: polyaniline, graphene, ferrocenecarboxylic acid, nitrite, electrochemical sensor

Introduction

Recently, the talking point was focused on harm impact of nitrite on human health, formed during the biodegradation of nitrate and ammoniacal nitrogen or nitrogenous organic matter.[1,2] Nitrite can interact with hemoglobin to form methemoglobin by oxidation of ferrous iron (Fe^{2+}) to the ferric state (Fe^{3+}), thus reduce the ability of blood to transport oxygen, which is described as methemoglobinemia that is dangerous, especially in infants (the so-called blue-baby syndrome).[3] Because the reaction between nitrite and secondary amines can result in the formation of carcinogenic, teratogenic, and mutagenic species, it can increase remarkably risk of the stomach cancer and esophagus cancer.[4] High concentration of nitrite assembled by fertilizers and/or polluted water sources was usually absorbed by the various vegetables. Many methods for nitrite determination have been developed in recent years, for example, spectrophotometry,[5-8] micro-spectrophotometry with liquid-phase microextraction,[9] capillary isotachophoresis,[10] microchip electrophoresis,[11] chromatography,[12] Raman spectroscopy,[13] gas chromatography-mass spectrometry (GC-MS),[14] electrochemical method,[15,16] etc. However, those methods often have some obvious disadvantages, such as higher cost owing to expensive apparatus, complicated operation and so on. Therefore, it is important to develop a simple and novel method with high efficiency and convenience for sensitive analysis of nitrite.

Graphene (GR) has become a well known material since it was first obtained by Geim using a mechanical exfoliation method in 2004.[17] The magic two-dimensional material has recently attracted a great deal of attention, because of its distinct characters, such as excellent electrical and

*e-mail: xbsfda123@126.com

physical properties, low cost, wide potential applications in electrics and sensors.[18,19] These unique properties had led to numerous efforts of applying graphene in electronic devices, such as supercapacitors,[20] solar cells[21] and lithium ion batteries.[22] At the same time, due to the nanostructure of graphene, it was widely applied as electrode material too.[23-25] High specific surface area and good electrical conductivity of the sheet like structure of graphene could effectively improve the sensitivity of the sensors based on the graphene and functionalized graphene modified electrodes.[16,26]

Ferrocene (Fc) and ferrocene derivatives (FD) are attracting keen interest of the electroanalysts for its unique redox behavior.[17] They could be used as mediators to increase the sensor sensitivity in FD and glucose oxidase (GOD) monomolecular film modified graphite electrodes.[27] At the same time, ferrocene and it derivatives, as perfect mediators, still possess other advantages such as low relative molar mass, good reversibility, fast reaction, high stability in both oxidized and reduced forms.[28] Ferrocenecarboxylic acid (FCA), the simplest carboxylic acid containing ferrocene group, incorporated in molecular and supramolecular structures has been used as electron transfer catalyst and molecular sensor,[29-32] which has also attracted much attention in the field of coordination chemistry due to its excellent properties including high thermal stability, excellent redox activity,[33] and enzymatic activity facilitation.[34] The basic unit of Fc, through a reversible oxidation process, generates the ferrocinium ion (Fc+), under mild potential conditions.[35] Moreover, FCA can dissolve in water and effectively promote the electron transfer rate, reduce the overpotential and remove the interferences of other electric active substances.[36] When the mixture of GR and FCA was dispensed on surface of the glass carbon electrode they can enhance the conductivity and electron-giving ability of the modified electrode, which is very advantageous for a redox reaction.

As FCA can improve dissolution of GR in aqueous solution, aniline was polymerized and deposited on the surface of the GR and FCA composite modified electrode to prevent the modified film from dissolving in the water. Moreover, polyaniline (PANI) coated on the GR and FCA composite modified electrode can still enhance its electrocatalytic property through accelerating the rate of heterogeneous electron transfer of the analyte. Besides, PANI film has a well doping and de-doping character of high conductivity and high specific surface area,[37,38] so it can be used in electrochemical sensors, electric condenser[39] and exchange membrane.[40] Aniline could be completely adsorbed by FCA to form a dense membrane during the polymerized reaction and to improve the modified electrode stability. Although there have been many studies about polyaniline-carbon nanotubes or polyaniline-graphene nanocomposites,[40-43] preparations of ferrocene/graphene/PANI composition materials and their application in the determination of nitrite have few been reported.

In this present work, a PANI/GR-FCA composite film modified electrode was fabricated by an electropolymerization of aniline on the GR-FCA modified glass carbon electrode. Cyclic voltammetry and differential pulse voltammetry were employed for highly sensitive determination of nitrite. Effects of polymerization cycles of aniline, buffer solution, pH, accumulation potential, accumulation time and scan rate on the determination on the PANI/GR-FCA/GCE modified electrode were investigated and discussed. The results indicated that the prepared modified electrode possessed high electrocatalytic activity and accumulative effect on nitrite determination.

Experimental

Reagents and apparatus

Natural graphite powder (< 20 μm) was purchased from Tianjin Guangfu Research Institute (Tianjin, China). Ferrocenecarboxylic acid was obtained from Shanghai Chemical Reagent Corporation (Shanghai, China). Aniline (≥ 99.5%, Shantou Xilong Chemical Factory, Guangdong, China) was distilled over zinc dust to remove the oxidation impurities prior to use. Hydrazine hydrate (50%), sodium nitrite, phosphoric acid, boric acid, glacial acetic acid, sodium hydroxide, sodium dihydrogen phosphate, dibasic sodium phosphate, potassium chloride, concentrated hydrochloric acid, concentrated sulfuric acid, sodium acetate, were of analytical reagent grade. Britton-Robinson buffer solution (BR) was prepared by mixing the 0.04 mol L^{-1} mixture of phosphoric acid, boric acid and acetic acid, and 0.2 mol L^{-1} sodium hydroxide to the proper pH. Other chemicals were of analytical grade and used as received. Double-distilled water was used throughout the experiments. Standard nitrite aqueous solutions were prepared daily.

All electrochemical experiments were carried out in a conventional three-electrode system controlled by CHI 660E electrochemisty workstation (Chenhua Instruments Co., Shanghai, China). A bare glass carbon electrode (GCE) or modified GCE was used as working electrode, a platinum sheet and a saturated calomel electrode (SCE) respectively served as the counter electrode and reference electrode at room temperature.

A JSM-6701 field emission scanning electron microscopy (SEM) (Japanese Electron Optics Company, Japan) was employed to observe the morphologies of the samples with

an acceleration voltage of 20 kV. Transmission electron microscope (TEM) images of the samples deposited on carbon-copper grids were taken on a JEM 1200EX microscope. Fourier transform infrared (FTIR) spectra were recorded on a Digilab FTS3000 FT-IR spectrometer using the KBr wafer technique. X-ray powder diffraction (XRD) patterns were obtained with an X'Pert/PRO diffractometer in the reflection mode using Cu Kα radiation source with a resolution of 0.02° and scanning speed of 0.5 degree min^{-1}. Unless otherwise stated, all experiments were carried out at room temperature.

Preparation of salted vegetable and urine samples

The treatment of salted vegetable samples was carried out according to the official procedure GB 5009.33-2010.[44] 50 g of the sample slurry was homogenized with 50 mL of distilled water in a 250 mL beaker. Then 12.5 mL of borax saturated solution was added in above mixture solution. After 50 mL of hot water (70 °C) was poured into the beaker it was heated (95 °C) for 15 min. After the solution was cooled to room temperature, 5 mL of $K_4Fe(CN)_6 \cdot 3H_2O$ (106 g L^{-1}) solution was added and shaken for 2 min, and then 5 mL of $Zn(CH_3COO)_2 \cdot 2H_2O$ (220 g L^{-1}) was added and shaken for 2 min to precipitate protein. After placed for 0.5 h, the mixture was filtrated in order to remove the upper fat, the filtrate was diluted to a volumetric flask of 250 mL with distilled water and analyzed immediately.

Urine samples were collected from volunteers using propene polymer (PP) one-time urine cup at early morning time. The samples were either used for analysis of nitrite immediately or stored at –20 °C until analysis. 0.4 g active carbon used as decoloring agent was added into 10 mL centrifuge tube with 5 mL urine sample, followed by mixing for 30 s. The urine sample was filtered with one piece of filter paper and collected with a new tube and then diluted to the volume of 5 mL with distilled water for further analysis.

Synthesis of graphene

Graphite oxide (GO) was prepared via a chemical oxidation of natural graphite according to Hummers method.[45] Briefly, 5 g of raw graphite powder was added to 98% H_2SO_4 (46 mL) and stirred for 30 min in an ice bath. Then 6 g of $KMnO_4$ was slowly added to the mixture solution under the temperature below 10 °C. After continuous vigorous agitation at 35 °C for 24 h, 50 mL of deionized water was gradually added to the mixture under vigorous stirring in 2 h at room temperature. At last, 50 mL of 30% H_2O_2 was added in above mixture and the color of the solution changed immediately from yellowish brown to golden yellow. The mixture was washed with 10% HCl and centrifugated repeatedly in order to remove the residual metal ions. Then, the sample was washed with deionized water and filtrated repeatedly until the pH of filtrate reached 4-5. After dried at 65 °C in a vacuum oven, GO product, flaky texture gray powders were obtained.

Graphene was prepared according to a slightly modified reference method.[46] Typically, 100 mg of GO was dispersed in 100 mL of deionized water and sonicated for 30 min to make sure that all GO were dissolved in water completely to obtain a clayblack homogeneous solution. Then, 1 mL of hydrazine monohydrate was added in above solution and the reaction mixture was kept in an oil bath at 95 °C for 24 h. The graphene was obtained by filtration and washed with water several times. The product was dried in a vacuum over at 80 °C for 24 h and used for further characterization.

Fabrication of the modified electrode

Prior to modification, bare GCE (3 mm, diameter) was polished to a mirror with 1.0 μm, 0.3 μm and 0.05 μm alumina slurry in sequence. After each polishing, it was rinsed with deionized water and sonicated in 1:1 HNO_3, 1:1 ethanol, and deionized water respectively for 5 min, and dried under a nitrogen stream. Then, the electrode was put in 1.0 mol L^{-1} H_2SO_4 and potentially scanned in the potential range from –1.0 to + 1.0 V (*versus* SCE) until a stable CV profile was gotten. Then 1.20 mg graphene was dispersed in 20 mL deionized water and then mixed with 20 mg ferrocenecarboxylic acid and sonicated for 1 h to form a homogenous mixture. 5 μL of the mixture was dropped on the pretreated GCE with a microsyringe, and then dried for 24 h in air before use.

The PANI/GR-FCA/GCE film modified electrode was formed by cyclically voltammetric scanning at 50 mV s^{-1} between –0.2 V and + 1.0 V (*versus* SCE) for twenty cycles in 0.02 mol L^{-1} aniline solution containing 0.5 mol L^{-1} H_2SO_4 though an electrochemical deposition method.[47] After electropolymerization, the modified electrode was washed with deionized water. Blue PANI was found to deposite on the surface of GR-FCA/GCE modified electrode.[48] After that, the resulting composite films were maintianed in potentiostatic mode at a potential of 1.0 V for 60 s and then at a potential of –0.2 V for 60 s in a solution containing 0.5 mol L^{-1} H_2SO_4 in order to remove any residual aniline monomer from the electrode surface. The obtained modified electrode was denoted as PANI/GR-FCA/GCE. For comparion, PANI/GCE electrode was also prepared with a similar process. The structure formula of polyaniline produced by an oxidation polymerization of aniline is illustrated in Scheme 1.

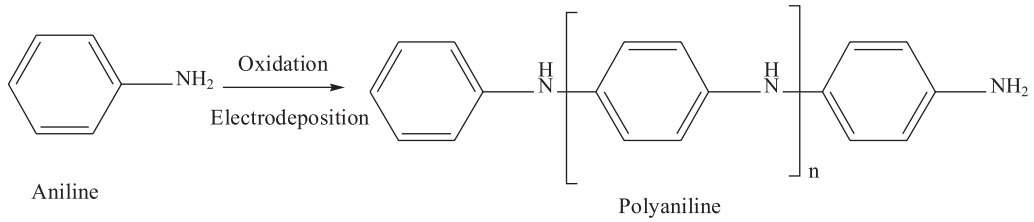

Scheme 1. The structure formula of polyaniline produced by the oxidation polymerization of aniline.

Results and Discussion

Structural characterizations of the electrode modified materials and the modified electrode

The morphologies of the graphene and corresponding PANI/GR-FCA composite film were studied by SEM and TEM and the results are shown in Figure 1, SEM image (Figure 1a) showed that the graphene sheets consisted of aggregated, crumpled, thin sheets in a random manner closely associated with each other to form a disordered structure. The corrugation and scrolling characteristics were intrinsic to graphene nanosheets.[49] This winkled nature of graphene was very beneficial to keeping a high specific surface area on the electrode. TEM image revealed that graphene sheet exhibited as an ultrathin transparent structure (Figure 1b). The transparent sheets were flake-like with wrinkles, which might be a key point leading to a gain in elastic energy for the quasi-two dimension crystallite to avoid dislocations caused by thermal fluctuations and keep a metastable state.[50]

Figure 1c shows the SEM morphology of the electropolymerized film. PANI film uniformly deposited on GR-FCA/GCE electrode and three-dimension network composite structures stood upright on electrode surface. The character was probably responsible for a high permeability and suitable permselectivity to determination of nitrite.

To confirm the structures and properties of graphene and graphene oxide, FTIR spectra of graphene, graphene oxide and graphite were measured and the results are shown in Figure 2. No obvious peak was detected on the pristine graphite except a broad band at 3440 cm^{-1}, which was assigned to the O–H stretching vibration of the intercalated water (Figure 2a). Figure 2b shows typical FTIR spectra of graphene oxide, the band at 1625 cm^{-1} was ascribed to C=C stretching vibration, and the bands around 3440, 1725, 1393, 1060 cm^{-1} respectively resulted from –OH stretching vibration, −C=O stretching vibration, −OH bending vibration and C–O–C stretching vibration. Existence of the oxygen-containing functional groups of graphene oxide confirmed the successful oxidation of graphite. After GO was reduced to GR, the C=O vibration band disappeared, the broad O–H stretching bands decreased dramatically (Figure 2c) and the weak peak at 1625 cm^{-1} still presented. These characteristics strongly suggested formation of high purity of grapheme.[51,52]

X-ray diffraction patterns exhibited evident structural changes during the chemical reduction process from pristine graphite to the graphene. Figure 3a shows the characteristic (002) diffraction peak of pristine graphite located at 26.4° and a very sharp and strong basal reflection indicated the highly crystalline nature of graphite. As oxidation proceeded, the intensity of the (002) diffraction line gradually weakened and finally disappeared. After chemical reduction with hydrazine, graphene oxide was reduced to graphene sheets with a characteristic peak at $2\theta = 23.02°$ (Figure 3b), which confirmed that the regular layered structure of pristine graphite had been destroyed.

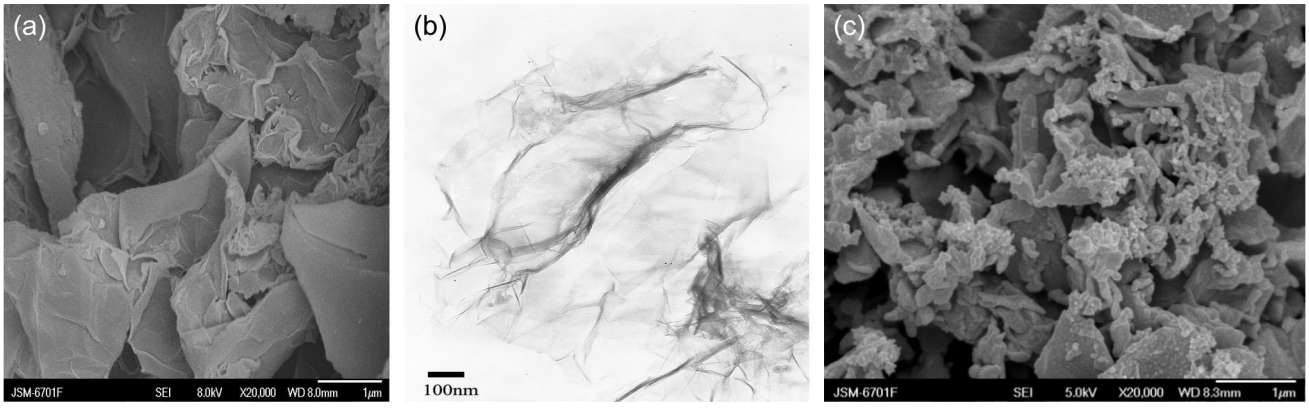

Figure 1. Morphological images of GR and the PANI/GR -FCA composite film. (a) SEM image of GR; (b) TEM image of GR; (c) SEM image of the PANI/GR -FCA composite film.

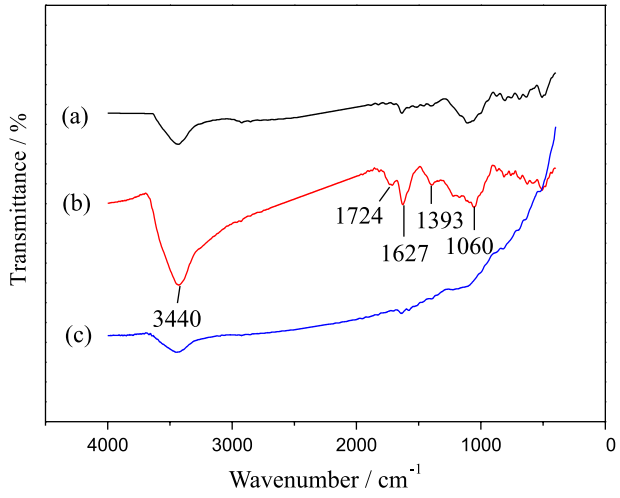

Figure 2. FTIR spectra of graphite(a); graphene oxide (b) and graphene (c).

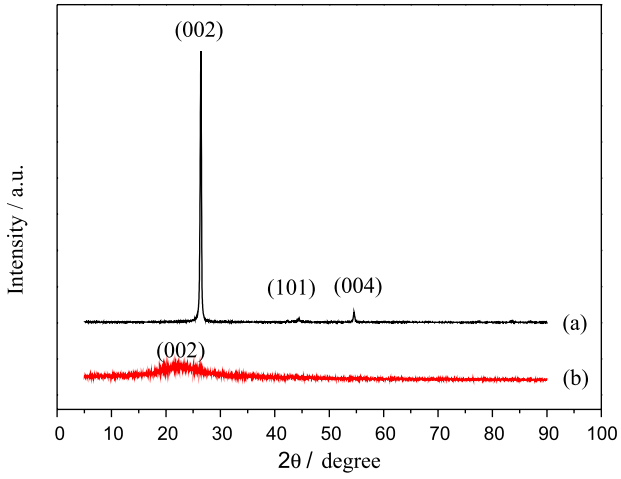

Figure 3. XRD patterns of graphite (a) and graphene (b).

The broad graphitic reflection of graphene indicated the graphene sheets were very thin.[53,54]

Electrochemical characteristics of the modified electrodes

Electrochemical impedance spectroscopy (EIS) was employed to monitor the modifying process of electrode, which is a power tool to probe the features of surface-modified electrode. EIS of different modified electrodes, GCE, PANI/GCE, and PANI/GR-FCA/GCE in the presence of equimolar $Fe(CN)_6^{3-/4-}$ containing 0.1 mol L^{-1} KNO_3 as supporting electrolyte were studied. The potential amplitude of ac was kept at 10 mV and the frequency range was set in the range of 0.1 Hz to 100 KHz. Figure 4 shows the Nyquist diagrams of different electrodes. A single semicircle in the high-frequency region and a straight line in the low-frequency region could be observed for all spectra. The bare GCE showed the biggest semicircle domain, which implied the highest electron-transfer resistance (Figure 4a). Comparing with curve a, semicircle diameter in curve b slightly decreased due to deposition of PANI on GCE (Figure 4b). Furthermore, EIS of the PANI/GR-FCA/GCE nanocomposite modified electrode had a remarkably decrease in diameter (Figure 4c), indicating the PANI/GR-FCA/GCE modified electrode had higher electrochemical activity and conductivity.

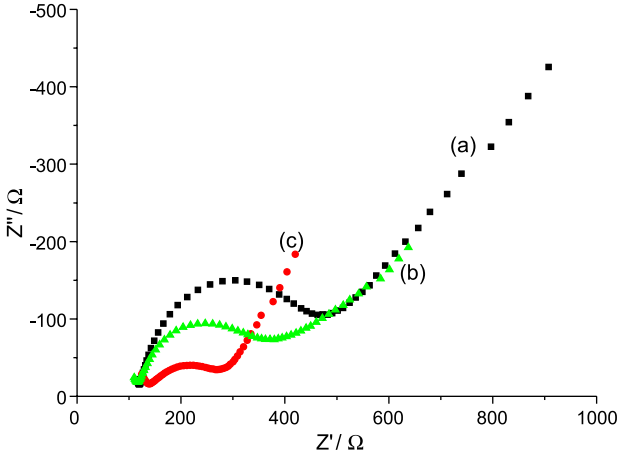

Figure 4. Electrochemical impedance spectroscopy of GCE (a); PANI/GCE (b); and PAN/GR-FCA/GCE (c) in 1.0 mmol L^{-1} $Fe(CN)_6^{3-/4-}$ solution containing 0.1 mol L^{-1} KNO_3 as supporting electrolyte. The frequency range was from 0.1 Hz to 100 KHz.

Figure 5 shows cyclic voltammograms recorded during electropolymerization of aniline on the GR-FCA/GCE film electrode. The currents on the cathodic and anodic waves increased with scanning times. And three pairs of redox peaks were observed, the two sets of peaks 0.207/0.069 V and 0.777/0.754 V were ascribed to transformations of leucoemeraldine/emeraldine and emeraldine/pernigraniline respectively, and third pair peaks in the middle 0.489/0.455 V was attributed to the defects in the linear structure of

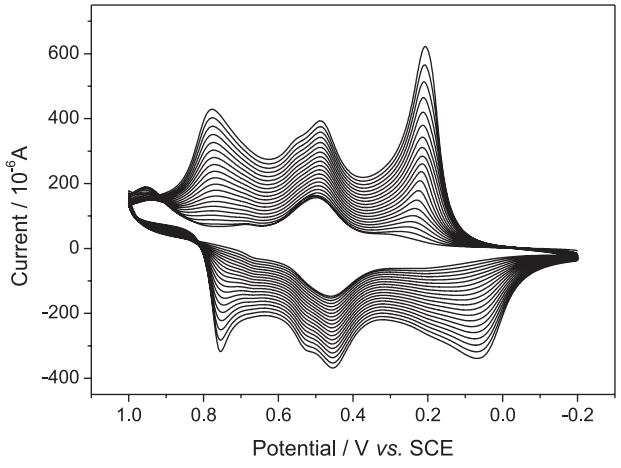

Figure 5. Cyclic voltammograms of 0.02 mol L^{-1} aniline solution containing 0.5 mol L^{-1} H_2SO_4 recorded at 50 mV s^{-1} during polymerization on the GR-FCA/GCE modified electrode.

PANI.[55,56] The multiple redox waves indicated complexity of the electro-oxidation of aniline, which involved both multiple heterogeneous electron transfer reactions and homogeneous chemical reactions resulted from different structures of the polyaniline film induced by different coupling processes between aniline cation radicals.[57] It also meant that aniline has been successfully polymerized in the GR-FCA/GCE modified electrode.

Electrochemical behavior of nitrite

The electrochemical behavior of nitrite was investigated by cyclic voltammetry (CV) in pH 4.0 BR buffer solution. Figure 6 shows the CVs of nitrite at the bare GCE, GR-FCA/GCE, PANI/GCE, PANI/GR-FCA/GCE. At the bare GCE (Figure 6a), there was only a very weak anodic peak at 0.936 V and the current of peak was 14.65 μA, which indicated that direct electron transfer of nitrite on bare GCE was very slow and irreversible. The peak current at PANI/GCE electrode (Figure 6b) slightly increased to 15.38 μA, and the potential shifted positively was 0.969 V. However, as shown in Figure 6c the GR-FCA/GCE electrode showed a poor response. It was because negatively charged ferrocenecarboxylate strongly repulsed the same charged nitrite ions and prevented them from permeating to the electrode surface in the pH 4.0 BR buffer solution. Interestingly, the PANI/GR-FCA/GCE modified electrode possessed the highest peak current 41.05 μA for oxidation of nitrite, which was approximately three times higher than that of the bare GCE, indicating that this modified electrode had an excellent electrocatalytic activity to nitrite oxidation. This phenomenon might be attributed to the electrostatic attraction of PANI and nitrite and excellent conductivity provided by grapheme, ferrocenecarboxylic acid and PANI composite.

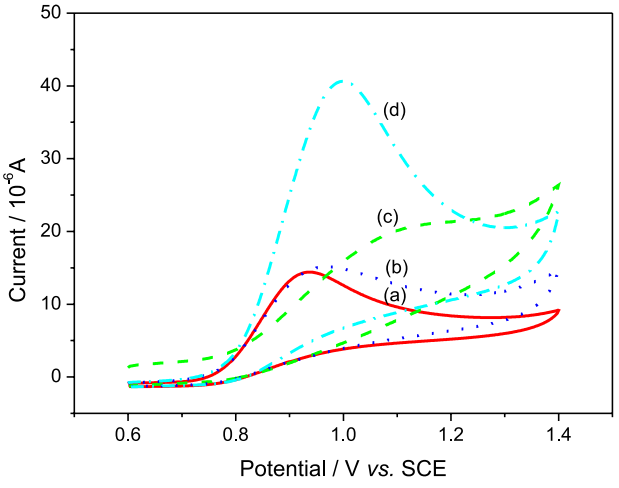

Figure 6. Cyclic voltammograms of 1 mmol L^{-1} nitrite respectively at the bare GCE (a); PANI/GCE(b); GR-FCA/ GCE (c); PANI/GR-FCA/ GCE(d) in the pH 4.0 BR buffer solution.

Effects of the experimental conditions on the oxidation currents of nitrite

Effects of polymerization cycles of aniline

Generally, the difference cycles of aniline polymerization defined the magnitude of the current response.[58] In the PANI modified electrode, the PANI thickness can be easily controlled by the polymerization cycles during the electropolymerization process. Figure 7 shows the response current change of 0.1 mmol L^{-1} nitrite in pH 4.0 BR buffer solution on the GR-FCA/GCE modified electrode with aniline polymerization cycles. As shown in Figure 7, the response current increased rapidly with the increment of polymerization cycles from 10 to 20 circles, indicating more and more polyaniline molecules were absorbed on the surface of the electrode, which led to an increase of the peak current. However, when the polymerization cycles exceeded 20, the response current decreased dramatically. So 20 was selected as the optimal polymerization cycles.

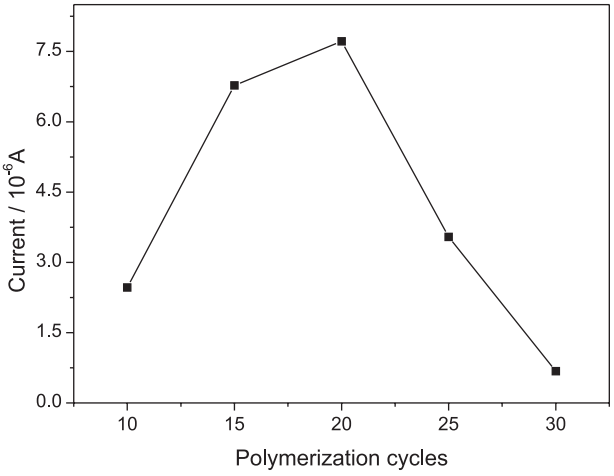

Figure 7. Effect of polymerization cycles of aniline on the oxidation currents of nitrite of 0.1 mmol L^{-1} in pH 4.0 BR buffer solution containing 0.02 mol L^{-1} aniline.

Selection of supporting electrolyte and pH value

The buffer solution possessed a significant influence on the response current of the modified electrode. Figure 8 shows cyclic voltammograms of 1.0 mmol L^{-1} nitrite on the PANI/GR-FCA/GCE in different media. From Figure 8, it could be seen that in pH 4.0, BR buffer solution nitrite had the strongest current response and the most negative oxidation potential. Therefore, BR buffer solution was selected as the working medium.

When proton took part in an electrochemical reaction, the solution acidity would greatly affect the reaction rate. In this present work, the influence of pH on the determination of nitrite was studied by different pulse voltammetry (DPV). Figure 9a shows that with pH increasing, the peak current

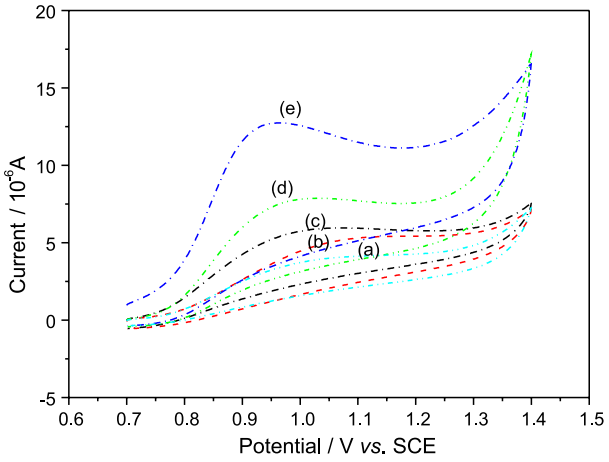

Figure 8. Cyclic voltammograms of 1 mmol L^{-1} nitrite on the PANI/GR-FCA composition film modified GCE electrode at 0.05 V s^{-1} scan rate and pH 4.0. (a) 0.1 mol L^{-1} H_2SO_4-NaOH solution; (b) 0.1 mol L^{-1} KCl-HCl solution; (c) 0.1 mol L^{-1} NaAc-HAc solution; (d) 0.1 mol L^{-1} NaH_2PO_4-Na_2HPO_4 solution; (e) BR buffer solution.

started to increase until pH 4.0 and then decreased, which indicated a weak acidic environment was necessary to obtain a good current response. It could be explained by the fact that the $–NH_2$ group was converted into $–NH_3^+$ at lower pH, which made it easy to absorb NO_2^-.[59] In addition, the peak potential of nitrite was found to linearly decrease with the pH value increasing from 2.0 to 6.0 with a regression equation E_{pa} (V) = 0.9448 – 0.0244pH (R^2 = 0.9961), suggesting involvement of proton in the electrode reaction (Figure 9b). According to above facts, pH 4.0 was chosen as an appropriate acidity condition for the determination of nitrite.

Effects of accumulation potential and accumulation time on the response of nitrite

The amount of adsorption of nitrite and the determination sensitivity can be improved, and the detection limit can be decreased by the accumulation of nitrite at the electrode. Effect of the accumulation potential on the voltammetric response of 0.25 mmol L^{-1} nitrite in pH 4.0 BR buffer solution at the modified electrode was examined in the potential range of –0.4 to 0.2 V and the result is shown in Figure 10a. The peak current of nitrite oxidation increased remarkably with the accumulation potential from –0.40 to –0.20 V, and then decreased gradually with the accumulation potential from –0.20 to 0.10 V. Therefore, the optimum accumulation potential was –0.2 V for determination of nitrite.

In addition, accumulation time also played an important role for pre-concentration of nitrite in pH 4.0 BR buffer solution. As shown in Figure 10b, the peak current increased rapidly with the accumulation time increasing and reached the maximum value at 90 s when the adsorption of nitrite saturated. So 90 s was chosen as an optimal accumulation time for further experiments.

Effect of the scanning rate

The effect of scan rate on the oxidation of nitrite was investigated with CV. Figure 11 shows the cyclic voltammograms of 1.0 mmol L^{-1} nitrite at different scan rates at the PANI/ GR-FCA/GCE modified electrode with the optimum conditions. The peak potentials for nitrite oxidation shifted positively with the increasing scan rate. The oxidation peak currents increased linearly with the scan rates in the range from 20 to 100 mV s^{-1}. The linear relationship between the peak current and scan rate could be expressed by the linear regression equation I_{pa} (μA) = 8.4921 + 0.0344υ (mV s^{-1}) (R^2 = 0.9972), which suggested that nitrite oxidation on the modified electrode was an adsorption-controlled process.

Determination of nitrite on the PANI/GR-FCA/GCE

On addition of nitrite, an obvious increase of the anodic peak current was observed, showing a

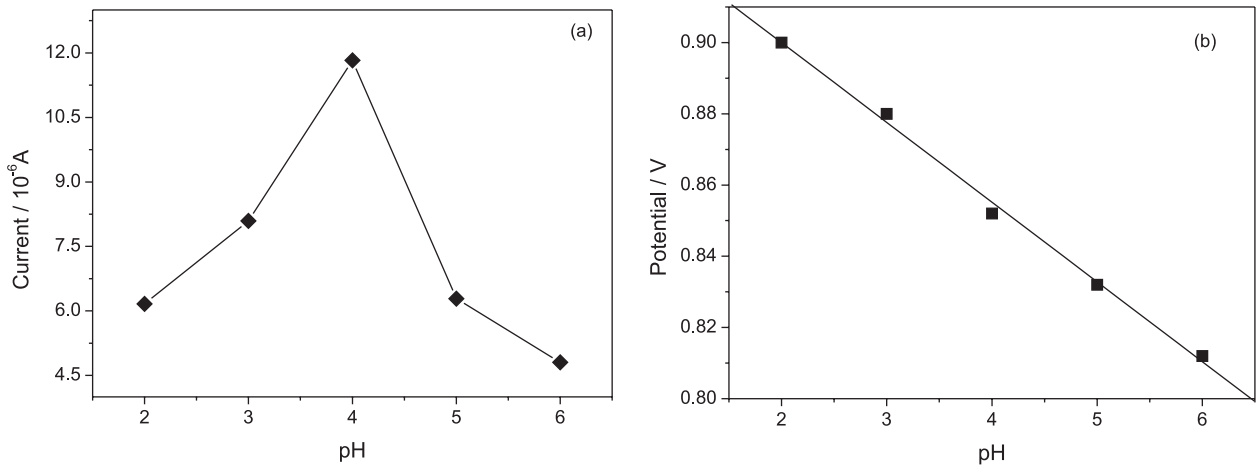

Figure 9. Effects of pH on the peak current (a) and peak potential (b) of 1 mmol L^{-1} nitrite in BR buffer solution.

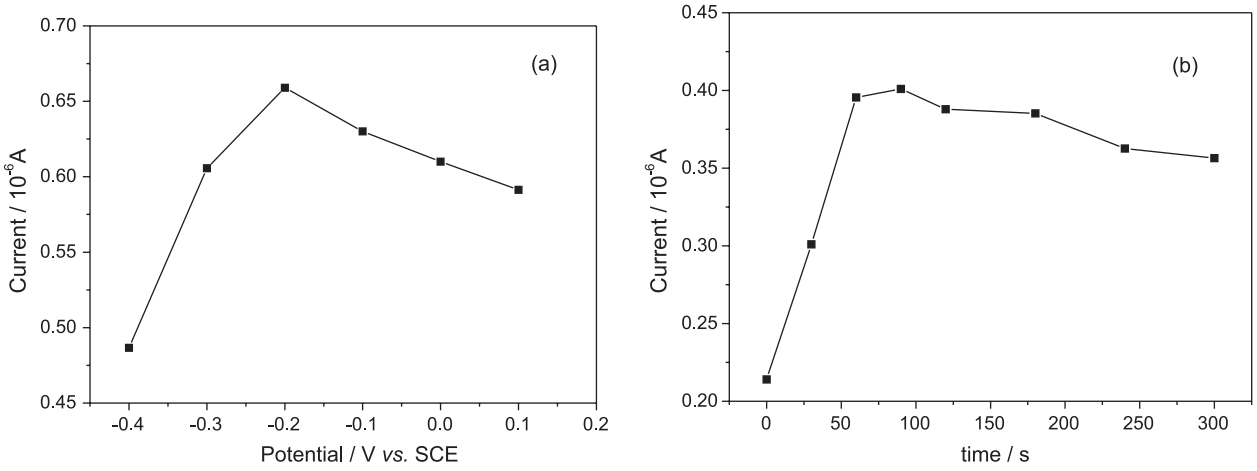

Figure 10. Effects of accumulation potential (a) and accumulation time (b) on the peak currents of 0.25 mmol L^{-1} nitrite.

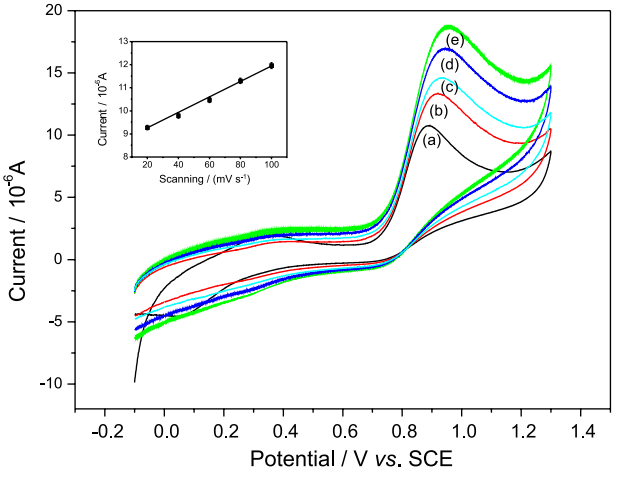

Figure 11. Cyclic voltammograms of 1.0 mmol L^{-1} nitrite at the PANI/GR-FCA/GCE modified electrode in pH 4.0 BR buffer solution at scan rates of (a) 20; (b) 40; (c) 60; (d) 80; (e) 100 mV s^{-1}. Inset: plot of peak current *vs*. the scan rate.

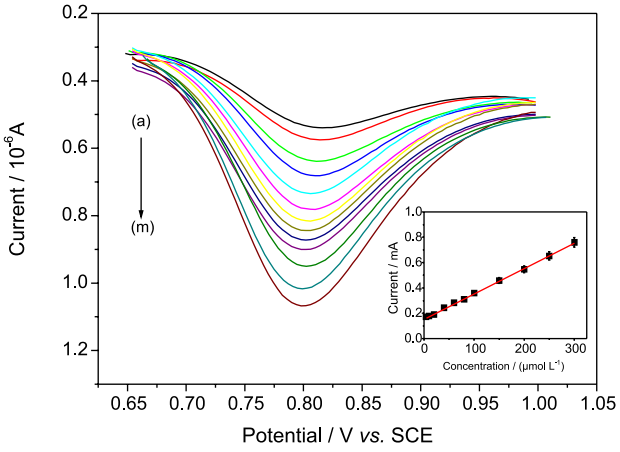

Figure 12. DPVs of the PANI/GR-FCA/GCE in pH 4.0 BR buffer solution containing different concentrations of nitrite from (a) to (m) were 4, 6, 8, 10, 20, 40, 60, 80, 100, 150, 200, 250, 300 μmol L^{-1}. Inset: corresponding linear calibration curve of peak current *vs.* nitrite concentration. Pulse amplitude: 50 mV, pulse width: 50 ms, pulse period: 0.2 s.

sensitive electrochemical response of nitrite on the PANI/GR-FCA/GCE. Figure 12 shows typical differential pulse voltammetric responses during successively adding 0.4 μmol L^{-1} ca. 300 μmol L^{-1} nitrite to 10 mL of the analytical solution containing 1 mL of pH 4.0 BR buffer. The peak current response for oxidation of nitrite increased linearly with the nitrite concentration increasing with a linear regression equation I (μA) = 0.1589 + 0.0020C (μmol L^{-1}) (R^2 = 0.9971, n = 13) and detection limit down to 0.02 μmol L^{-1} (S/N = 3).

Possible interferences for the nitrite detection on the PANI/GR-FCA modified GCE were studied by DPV through adding various amounts of interference ions into the pH 4.0 BR buffer solution containing 0.3 mmol L^{-1} nitrite. The results showed that 150-fold excess of K^+, Na^+, Mg^{2+}, NH_4^+, Cl^-, SO_4^{2-}, NO_3^-, CO_3^{2-}, CH_3COO^-, F^-, Br^-, SO_3^{2-}, ClO_4^-, I^-, SCN^-, benzoate, 100-fold excess of Ba^{2+}, Ca^{2+}, Zn^{2+}, glucose, ClO_3^-, 50-fold excess of Al^{3+}, $Cr_2O_7^{2-}$, L-glutamic acid and ascorbic acid had no interference on the current response of nitrite, whereas Ni^{2+}, Cu^{2+}, Fe^{3+} were found to possessed serious interferences. 5-fold excess of Ni^{2+}, Cu^{2+} and Fe^{3+} would yield 5% of relative error. However, their interferences could be easily eliminated by adding 1 mL of 0.01 mol L^{-1} EDTA as a masking agent. So, the proposed method had an excellent selectivity for the determination of nitrite.

In order to validate the viability, the proposed method was applied successfully for the determination of nitrite in healthy human urine and salted vegetable samples. Recovery studies were carried out by the standard addition method to eliminate any matrix effect. Table 1 summarizes the results obtained for the vegetable and human urine real samples. The recoveries of all determinations ranged between 96-102%, and RSD (n = 5) was less than 4.8%.

Table 1. Determination of nitrite in salted vegetable

Sample	Added / (μmol L^{-1})	Found / (μmol L^{-1})	Recovery / %	RSD / % (n = 5)
Salted vegetable	30	29.74	99	4.8
	50	50.37	101	3.9
	100	102.10	102	1.8
Urine	0	0.85	–	4.8
	0.50	1.33	96	3.8
	1.00	1.87	102	1.2

RSD: relative standard deviation.

The proposed method gave a sensitive and selective electrochemical response for the determination of nitrite ion that could be used to real samples. The sensitivity, linear range and detection limit were as good as or better than some of the previously reported methods. Table 2 shows a comparison of the developed method with some of the previously methods in literatures.

Stability and reproducibility of the modified electrode

Stability and reproducibility of the modified electrode were investigated by repeatedly examining the response current to nitrite. The modified electrode possessed a good repeatability for nitrite determination. The relative standard deviation (RSD) for 15 determinations of 0.10 mmol L^{-1} nitrite at the same modified electrode was 2.09%. To test the reproducibility of the modified electrode, the response current to nitrite at five electrodes prepared in the same way was recorded at pH 4.0 BR buffer with 0.10 mmol L^{-1} nitrite and it was found the RSD was 3.45%. When a modified electrode was stored at 4 °C in a refrigerator for 25 days, its current response still maintained 96.24% of its initial value. The excellent long-term stability could be attributed to the stability of the PANI/GR-FCA composite film.

Conclusions

In this present work, a simple, low-cost and convenient method for preparation of the PANI/GR-FCA composite film modified glass carbon electrode was proposed. The modified electrode showed a high electrochemical activity towards the oxidation of nitrite and could be used as a sensitive electrochemical sensor for the differential pulse voltammetric determination of nitrite with satisfactory results. When the nitrite concentration was in the range of 0.4 μmol L^{-1} ca. 300 μmol L^{-1} the peak current response for oxidation of nitrite increased linearly with the nitrite concentration increasing with a linear regression equation I (μA) = 0.1589 + 0.0020C (μmol L^{-1}) (R^2 = 0.9971, n = 13) and the detection limit was down to 0.02 μmol L^{-1} (S/N = 3). And the recoveries of all determinations ranged between 96-102%.

Acknowledgements

This work was supported in part by the National Nature Science Foundation (20873101) and Key Lab of Eco-environment Related Polymer Materials of MOE, and Key Lab of Bioelectrochemistry and Environmental Analysis of Gansu Province, Northwest Normal University, China.

Table 2. Comparison of the proposed method with some of the methods reported in literature

Method	Linear range	Limit of detection	Reference
Fluorimetry	0.87-1.7 μmol L^{-1}	0.30 μmol L^{-1}	60
Cyclic voltammetry	1-160 μmol L^{-1}	1 μmol L^{-1}	61
Voltammetry	30-1000 μmol L^{-1}	28 μmol L^{-1}	62
Amperometry	10-1000 μmol L^{-1}	2.3 μmol L^{-1}	48
	5-500 μmol L^{-1}	1.4 μmol L^{-1}	
Amperometry	5.0-150 μmol L^{-1}	1.0 μmol L^{-1}	58
Differential pulse voltammetry	0.50-100 μmol L^{-1}	0.10 μmol L^{-1}	59
Amperometry	0.13-44 mmol L^{-1}	45 μmol L^{-1}	63
Micelle mediated cloud extraction-spectrophotometry	0.17-2.61 μmol L^{-1}	0.13 μmol L^{-1}	64
Spot test/diffuse reflectance spectroscopy	6.3-108 μmol L^{-1}	1.96 μmol L^{-1}	65
Fluorimetry	10-350 nmol L^{-1}	0.20 nmol L^{-1}	66
Differential pulse voltammetry	0.4 μmol L^{-1} ca. 300 μmol L^{-1}	0.02 μmol L^{-1}	This work

References

1. Mikuška, P.; Vecera, Z.; *Anal. Chim. Acta* **2003**, *495*, 225.
2. Chan, T. Y. K.; *Toxicol. Lett.* **2011**, *200*, 101.
3. Özdestan, Ö.; Üren, A.; *J. Agric. Food Chem.* **2010**, *58*, 5235.
4. Bories, P. N.; Bories, C.; *Clin. Chem.* **1995**, *41*, 904.
5. Al-Okab, R. A.; Syed, A. A.; *Talanta* **2007**, *72*, 1239.
6. Shariati-Rad, M.; Irandoust, M.; Mohammadi, S.; *Spectrochim. Acta, Part A* **2015**, *149*, 190.
7. Schnetger, B.; Lehners, C.; *Mar. Chem.* **2014**, *160*, 91.
8. García-Robledo, E.; Corzo, A.; Papaspyrou, S.; *Mar. Chem.* **2014**, *162*, 30.
9. Senra-Ferreiro, S.; Pena-Pereira, F.; Lavilla, I.; Bendicho, C.; *Anal. Chim. Acta* **2010**, *668*, 195.
10. Jastrzębska, A.; *J. Food Compos. Anal.* **2011**, *24*, 1049.
11. Troška, P.; Chudoba, R.; Danč, L.; Bodor, R.; Horčičiak, M.; Tesařová, E.; Masár, M.; *J. Chromatogr. B* **2013**, *930*, 41.
12. Vanatta, L. E.; *J. Chromatogr. A* **2008**, *1213*, 70.
13. Zhang, K.; Hu, Y. L.; Li, G. K.; *Talanta* **2013**, *116*, 712.
14. Pagliano, E.; Meija, J.; Mester, E.; *Anal. Chim. Acta* **2014**, *824*, 36.
15. Wang, S. Q.; Lin, X. Q.; *Electrochim. Acta* **2005**, *50*, 2887.
16. Radhakrishnan, S.; Krishnamoorthy, K.; Sekar, C.; Wilson, J.; Kim, S. J.; *Appl. Catal., B* **2014**, *148-149*, 22.
17. Huang, K. J.; Miao, Y. X.; Wang, L.; Gan, T.; Yu, M.; Wang, L. L.; *Process Biochem.* **2012**, *47*, 1171.
18. Krishnamoorthy, K.; Kim, G. S.; Kim, S. J.; *Ultrason. Sonochem*. **2013**, *20*, 644.
19. Niu, X. L.; Yang, W.; Guo, H.; Ren, J.; Gao, J. Z.; *Biosens. Bioelectron*. **2013**, *41*, 225.
20. Sun, D. F.; Yan, X. B.; Lang, J. W.; Xue, Q. J.; *J. Power Sources* **2013**, *222*, 52.
21. Miao, X. C.; Tongay, S.; Petterson, M. K.; Berke, K.; Rinzler, A. G.; Appleton, B. R.; Hebard, A. F.; *Nano Lett.* **2012**, *12*, 2745.
22. Wu, Z. S.; Ren, W. C.; Xu, L.; Li, F.; Cheng, H. M.; *ACS Nano* **2011**, *5*, 5463.
23. Stankovich, S.; Dikin, D. A.; Dommett, G. H. B.; Kohlhaas, K. M.; Zimney, E. J.; Stach, E.; Piner, R. D.; Nguyen, S. T.; Ruoff, R. S.; *Nature* **2006**, *442*, 282.
24. Cassagneau, T.; Guerin, F.; Fendler, J. H.; *Langmuir* **2000**, *16*, 7318.
25. Niu, X. L.; Yang, W.; Guo, H.; Ren, J.; Yang, F.; Gao, J. Z.; *Talanta* **2012**, *99*, 984.
26. Radhakrishnan, S.; Krishnamoorthy, K.; Sekar, C.; Wilson, J.; Kim, S. J.; *Chem. Eng. J.* **2015**, *259*, 594.
27. Barmin, A. V.; Eremenko, A. V.; Kurochkin, I. N.; Sokolovsky, A. A.; *Electroanalysis* **1994**, *6*, 107.
28. Raoof, J. B.; Ojani, R.; Kolbadinezhad, M.; *Electroanalysis* **2005**, *17*, 2043.
29. Sabapathy, R. C.; Bhattacharyya, S.; Leavy, M. C.; Cleland Jr., W. E.; Hussey, C. L.; *Langmuir* **1998**, *14*, 124.
30. Carollo, L.; Curulli, A.; Floris, B.; *Appl. Organomet. Chem.* **2003**, *17*, 589.
31. Ndamanisha, J. C.; Guo, L. P.; Wang, G.; *Microporous Mesoporous Mater.* **2008**, *113*, 114.
32. Zhu, C. C.; Yang, L. G.; Li, D. C.; Zhang, Q. F.; Dou, J. M.; Wang, D. Q.; *Inorg. Chim. Acta* **2011**, *375*, 150.
33. Ndamanisha, J. C.; Guo, L. P.; *Biosens. Bioelectron.* **2008**, *23*, 1680.
34. Bartlett, P. N.; Bradford, V. Q.; Whitaker, R. G.; *Talanta* **1991**, *38*, 57.
35. Fernandez, L.; Carrero, H.; *Electrochim. Acta* **2005**, *50*, 1233.
36. Huang, X. J.; Im, H. S.; Lee, D. H.; Kim, H. S.; Choi, Y. K.; *J. Phys. Chem. C* **2007**, *111*, 1200.
37. Gu, B.; Brown, G. M.; Chiang, C. C.; *Environ. Sci. Technol.* **2007**, *42*, 6277.
38. Bhadra, S.; Khastgir, D.; Singha, N. K.; Lee, J. H.; *Prog. Polym. Sci.* **2009**, *34*, 783.
39. Qu, F. L.; Yang, M. H.; Jiang, J. H.; Shen, G. L.; Yu, R. Q.; *Anal. Biochem.* **2005**, *344*, 108.
40. Gao, M. M.; Yang, Y.; Diao, M. H.; Wang, S. Q.; Wang, X. H.; Zhang, G. H.; Zhang, G.; *Electrochim. Acta* **2011**, *56*, 7644.
41. Wang, D. W.; Li, F.; Zhao, J. P.; Ren, W. C.; Chen, Z. G.; Tan, J.; Wu, Z. S.; Gentle, I.; Lu, G. Q.; Cheng, H. M.; *ACS Nano* **2009**, *3*, 1745.
42. Fan, Y.; Liu, J. H.; Yang, C. P.; Yu, M.; Liu, P.; *Sens. Actuators, B* **2011**, *157*, 669.
43. Wu, K. B.; Hu, S. S.; *Carbon* **2004**, *42*, 3237.
44. Institute of China Standards, *National Food Safety Standard: Determination of Nitrite and Nitrate in Foods*, GB 5009.33-2010, 2010.
45. Stankovich, S.; Dikin, D. A.; Piner, R. D.; Kohlhaas, K. A.; Kleinhammes, A.; Jia, Y. Y.; Wu, Y.; Nguyen, S. T.; Ruoff, R. S.; *Carbon* **2007**, *45*, 1558.
46. Niu, X. L.; Yang, W.; Ren, J.; Guo, H.; Long, S. J.; Chen, J. J.; Gao, J. Z.; *Electrochim. Acta* **2012**, *80*, 346.
47. Cai, L. T.; Chen, H. Y.; *J. Appl. Electrochem*. **1998**, *28*, 161.
48. Huang, X.; Li, Y. X.; Chen, Y. L.; Wang, L.; *Sens. Actuators, B* **2008**, *134*, 780.
49. Meyer, J. C.; Geim, A. K.; Katsnelson, M. I.; Novaseov, K. S.; Booth, T. J.; Roth, S.; *Nature* **2007**, *446*, 60.
50. Geim, A. K.; Novoselov, K. S.; *Nat. Mater.* **2007**, *6*, 183.
51. Guo, H. L.; Wang, X. F.; Qian, Q. Y.; Wang, F. B.; Xia, X. H.; *ACS Nano* **2009**, *3*, 2653.
52. Zhou, M.; Zhai, Y. M.; Dong, S. J.; *Anal. Chem.* **2009**, *81*, 5603.
53. Wang, G. X.; Yang, J.; Park, J.; Gou, X.; Wang, B.; Liu, H.; Yao, J.; *J. Phys. Chem. C* **2008**, *112*, 8192.
54. Subrahmanyam, K. S.; Vivekchand, S. R. C.; Govindaraj, A.; Rao, C. N. R.; *J. Mater. Chem.* **2008**, *18*, 1517.
55. Yang, H. J.; Bard, A. J.; *J. Electroanal. Chem.* **1992**, *339*, 423.
56. Zhang, L.; Zhang, C. H.; Lian, J. Y.; *Biosens. Bioelectron.* **2008**, *24*, 690.

57. Genies, E. M.; Tsintavis, C.; *J. Electroanal. Chem.* **1986**, *200*, 127.
58. Guo, M. L.; Chen, J. H.; Li, J.; Tao, B.; Yao, S. Z.; *Anal. Chim. Acta* **2005**, *532*, 71.
59. Jiang, L. Y.; Wang, R. X.; Li, X. M.; Jiang, L. P.; Lu, G. H.; *Electrochem. Commun.* **2005**, *7*, 597.
60. Guo, Y. X.; Zhang, Q. F.; Shangguang, X. C.; Zhen, G. D.; *Spectrochim. Acta, Part A* **2013**, *101*, 107.
61. Wu, Q.; Storrier, G. D.; Pariente, F.; Wang, Y.; Shapleigh, J. P.; Abruña, H. D.; *Anal. Chem.* **1997**, *69*, 4856.
62. Ojani, R.; Rahmanifar, M. S.; Naden, P.; *Electroanalysis* **2008**, *20*, 1092.
63. Liu, Y.; Gu, H. Y.; *Microchim. Acta* **2008**, *162*, 101.
64. Pourreza, N.; Fathi, M. R.; Hatami, A.; *Microchem. J.* **2012**, *104*, 22.
65. Luiz, V. H. M.; Pezza, L.; Pezza, H. R.; *Food Chem.* **2012**, *134*, 2546.
66. Liu, Q. H.; Yan, X. L.; Guo, J. C.; Wang, W. H.; Li, L.; Yan, F. Y.; Chen, L. G.; *Spectrochim. Acta, Part A* **2009**, *73*, 789.

Submitted: April 20, 2015
Published online: July 24, 2015